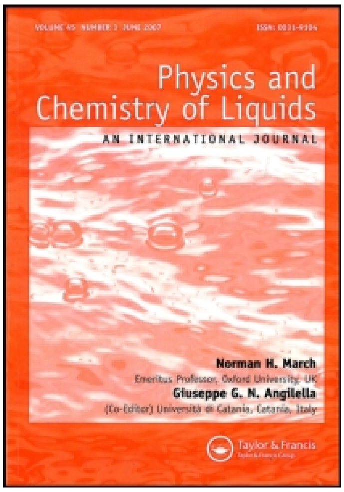

Physics and Chemistry of Liquids
Publication details, including instructions for authors and subscription information:
http://www.informaworld.com/smpp/title~content=t713646857

Electron (Hole) Liquids Flowing Through Both Heavy Fermion and Cuprate Materials in Superconducting and Normal States

G. G. N. Angilella[a]; N. H. March[bc]; R. Pucci[a]
[a] Dipartimento di Fisica e Astronomia, Università degli Studi di Catania, and Istituto Nazionale per la Fisica della Materia, Sezione di Catania, Catania, Italy [b] Oxford University, Oxford, England [c] Department of Physics, University of Antwerp (RUCA), Antwerp, Belgium

To cite this Article Angilella, G. G. N. , March, N. H. and Pucci, R.(2001) 'Electron (Hole) Liquids Flowing Through Both Heavy Fermion and Cuprate Materials in Superconducting and Normal States', Physics and Chemistry of Liquids, 39: 4, 405 — 427
To link to this Article: DOI: 10.1080/00319100108031673
URL: http://dx.doi.org/10.1080/00319100108031673

Phys. Chem. Liq., 2001, Vol. 39, pp. 405–427
Reprints available directly from the publisher
Photocopying permitted by license only

ELECTRON (HOLE) LIQUIDS FLOWING THROUGH BOTH HEAVY FERMION AND CUPRATE MATERIALS IN SUPERCONDUCTING AND NORMAL STATES

G. G. N. ANGILELLA[a,*], N. H. MARCH[b,c] and R. PUCCI[a]

[a]*Dipartimento di Fisica e Astronomia, Università degli Studi di Catania, and Istituto Nazionale per la Fisica della Materia, Sezione di Catania, Corso Italia, 57, I-95129 Catania, Italy;*
[b]*Oxford University, Oxford, England;*
[c]*Department of Physics, University of Antwerp (RUCA), Antwerp, Belgium*

(Received 9 August 2000)

In earlier work, we have considered electron (hole) liquids flowing through assemblies with antiferromagnetic fluctuations in the normal state of high-T_c cuprates. The present review has as its focus to compare and contrast these high-T_c cuprates with heavy Fermion superconductors. Both classes of materials will be considered in superconducting as well as in normal phases. In the former phase, a further focal point will be the symmetry of the pairing. In underdoped cuprates with *d*-wave symmetry, evidence continues to mount for preformed (2*e*) Bosons in the normal state, especially from neutron scattering experiments. This is in marked contrast to the heavy Fermion material UBe_{13}, where very recent differential conductivity measurements on a UBe_{13}–Au junction appear to exclude the formation of such precursor Bosons.

Keywords: Non–*s*-wave pairing superconductors; Heavy Fermion materials; High-T_c cuprates

I. BACKGROUND AND OUTLINE

While two groups of superconducting materials, namely BCS low-T_c metals and metallic alloys and materials like K_3C_{60} based on fullerene,

*Corresponding author.

are by now well understood [1, 2], the non $-s$-wave paired superconductors present still major unsolved problems. Therefore, in this review, we shall compare and contrast the unconventional superconductors in the high-T_c cuprates [3] and in heavy Fermion materials [4, 5]. In particular, it will be instructive to focus on the behaviour of electron (hole) liquids flowing through these two classes of materials in both normal and superconducting phases.

Two issues will provide the major focal points of the present overview:

(i) What determines the energy scale of the superconducting transition temperatures T_c in the heavy Fermion materials with very low transition temperatures and in the high-T_c cuprates, and
(ii) What is the evidence for precursor Boson formation in the normal state of the non $-s$-wave paired superconductors?

Issue (i) will be dealt with in Sec. II below, while Sec. III will be concerned with the second issue. In this latter context, it is highly relevant to refer to the more extensive review of Timusk and Statt [6], which provides essential background for the 'up-dating' given in Sec. III below. Section IV deals with theoretical issues raised on energy gaps in the superconducting state by non $-s$-wave pairing schemes, and summarizes briefly recent relevant experimental data [7] on UBe_{13}. Section V constitutes a summary.

II. ENERGY SCALES FOR T_c IN BOTH HEAVY FERMION MATERIALS AND IN CUPRATE SUPERCONDUCTORS

Elsewhere, we have presented evidence that the thermal energy $k_B T_c$ corresponding to the superconducting transition T_c shows a marked correlation with another energy scale [8], termed ε_c, and defined by

$$\varepsilon_c = \frac{\hbar^2}{m^* \xi^2}, \tag{1}$$

where m^* is the effective mass and ξ is the coherence length. We must note at this point that in work almost a decade ago, Uemura *et al.* [9] already focussed on the inverse effective mass m^* in forming an energy scale. However, they did not discuss the coherence length ξ in that context.

Following Ref. [8], we have plotted available data on six heavy Fermion materials in Figure 1, where the ordinate shows $k_B T_c$ and the *abscissa* is ε_c defined in Eq. (1). The dashed curve is mainly a guide to the eye, behaving as $k_B T_c \approx 21\varepsilon_c$ at low ε_c.

The important point to stress here is that $\varepsilon_c/k_B T_c$ for the three heavy Fermion materials with the lowest T_c values in Figure 1 is a small number of the order of 1/20. We have therefore proposed for heavy Fermion (hF) superconductors that

$$k_B T_c = f_{hF}\left(\frac{\hbar^2}{m^* \xi^2}\right), \tag{2}$$

where $f_{hF}(\varepsilon_c) \propto \varepsilon_c$, with a proportionality constant of ~ 20 for ε_c sufficiently small, but shows a tendency to saturate, *i.e.*, $f_{hF} \to$ const., at larger ε_c.

While we were able to find simultaneously values of T_c, m^*, and ξ for the six heavy Fermion materials, the situation is less favourable for the high-T_c cuprates. However, there is enough data to allow the log–log plot to be made in Figure 2, where it can be seen, in marked contrast to

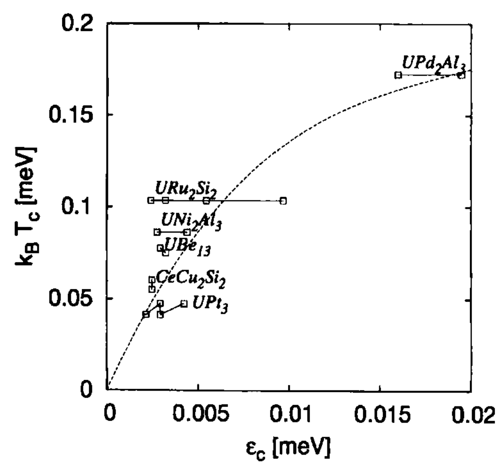

FIGURE 1 Thermal energy $k_B T_c$ corresponding to superconducting transition T_c *versus* characteristic energy $\varepsilon_c = \hbar^2/(m^* \xi^2)$, with m^* the effective mass and ξ the coherence length (see Ref. [8]). Six heavy Fermion materials are considered. Fitted (dashed) curve should be regarded mainly as a guide to the eye.

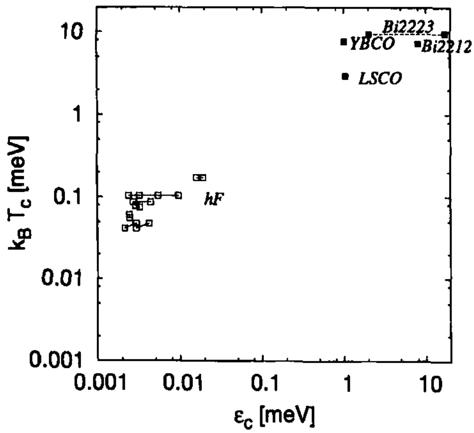

FIGURE 2 Log–log plot of Figure 1, but now with high-T_c cuprates in top-right hand corner (data taken from Poole *et al.*, Ref. [3]), in addition to heavy Fermion data of Figure 1 (here collectively marked by 'hF'). For the cuprates, use has been made of the coherence length ξ_{ab}. See also Ref. [8].

the heavy Fermion materials, that in order of magnitude $k_B T_c \sim \hbar^2/(m^* \xi^2)$. We shall return to this matter briefly in Sec. III.2.

III. EVIDENCE FOR PRECURSOR (2*e*) BOSON PAIRING IN HIGH-T_c CUPRATES AND THE CONTRAST WITH HEAVY FERMION MATERIALS

In relatively early work, Egorov and March [10, 11] started out from the two dimensional Fermi liquid study of Kohno and Yamada [12]. These authors relate two apparently very different physical quantities, the electrical resistivity ρ_a and the nuclear spin-lattice relaxation time T_1, to the magnetic susceptibility $\chi(\mathbf{Q})$ when carriers flow through assemblies with antiferromagnetic correlations as in the underdoped cuprates. Here, $\mathbf{Q}$ is the antiferromagnetic wave vector, and Egorov and March eliminated the susceptibility $\chi(\mathbf{Q})$ to obtain the prediction for the normal state of underdoped cuprates:

$$\rho_a T_1 \propto T. \tag{3}$$

Data for both ρ_a and T_1 have been taken from experiment for two materials for which both quantities have been measured over an appropriate temperature range [13, 14]. Their results for $YBa_2Cu_4O_8$ are reproduced in Figure 3. It is clear that there is an appreciable range of temperature over which the result of Eq. (3) is well borne out. But a new and major feature appears at a temperature of ~ 100 K, where the Hall coefficient and the thermoelectric power also exhibit anomalous behaviour as also discussed by Egorov *et al.* [10, 15]. This plot in Figure 3 can be interpreted as revealing a cross-over from Fermi liquid behaviour in Eq. (3) to a new phase of the carrier liquid in the lower temperature range. Angilella, March and Pucci [16] have discussed this further, and their work supports the interpretation of Egorov and March [10] that (2*e*) Boson pairs are formed in the normal state of this underdoped cuprate with a binding energy of $\sim (1/100)$ eV. The picture then of a mixture of (2*e*) Bosons and (*e*) Fermions in thermal equilibrium in this material below 100 K has been pressed by Chiofalo *et al.* [17], and is altogether consistent with such precursor Boson formation.

III.1. Evidence of Magnetic Correlation Above T_c from Neutron Scattering Experiments

To conclude this update of the review of Timusk and Statt [6] relating to precursor Bosons in the underdoped cuprates, it is important to emphasize the central role being played by neutron scattering experiments. As one important example, we shall choose to focus on

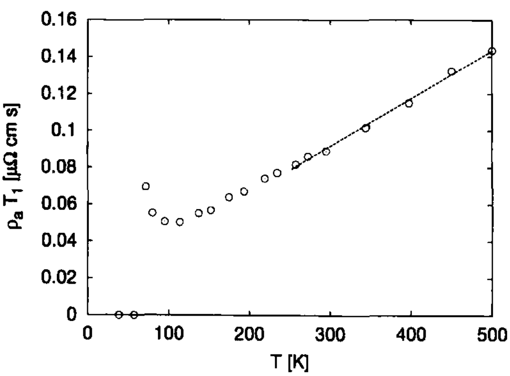

FIGURE 3 Plot of $\rho_a T_1$ *versus* temperature T for $YBa_2Cu_4O_8$ in the normal state. Redrawn from Egorov and March, Ref. [10]. Dashed line is the linear fit given by Eq. (A2) at $T \gg T_c$.

the very recent study of Dai *et al.* [18], which stresses the connection between superconducting phase correlations and short-range antiferromagnetic correlations in the cuprates. Specifically, these authors study $YBa_2Cu_3O_{6+x}$, where x controls the level of the hole-doping. As they emphasize, in this material the most prominent feature in the spectrum of magnetic (spin) excitations is the observation of a resonance, first recorded to our knowledge by Rossat-Mignod *et al.* [19] and later by other authors (see references in Dai *et al.* [18]). The achievement of the neutron scattering experiments of Dai *et al.* [18] is to show that, for underdoped $YBa_2Cu_3O_{6.6}$, modest magnetic fields tend to significantly suppress this resonance. This is especially the case for magnetic fields nearly perpendicular rather than parallel to the CuO_2 planes. Dai *et al.* [18] propose from these neutron measurements that the resonance is a fingerprint of pairing and phase coherence, and their results can leave little doubt that, as already stressed above in this review, magnetism plays a quite central role in the high-T_c cuprates. But in the present context, the further point they emphasize is that the persistence of such a magnetic field effect above T_c favours preformed pairs in the normal state of underdoped cuprates.

We shall turn next to confront this picture of precursor (2*e*) Bosons in underdoped cuprates with a very recent experiment on the heavy Fermion material UBe_{13}.

III.2. Differential Conductivity Measurement for a UBe_{13}–Au Junction

Wälti *et al.* [7] very recently have reported measurements of the differential conductivity of UBe_{13}–Au contact junctions. These are interpreted by these workers as revealing the existence of low-energy Andreev surface bound states. Their conclusion from their observation of huge conductance peaks at zero bias is supporting the view that UBe_{13} is an unconventional superconductor with nontrivial energy-gap symmetry (see also Sec. IV below).

Their results for the differential conductivity have been reconstructed in Figure 4. The point we wish to emphasize in the context of the present section is that the peaks in the superconducting state, *i.e.*, with $T_c < 0.90\,K$ in UBe_{13}, have disappeared in the normal state (lowest two curves in Fig. 4). Our interpretation (see also the related,

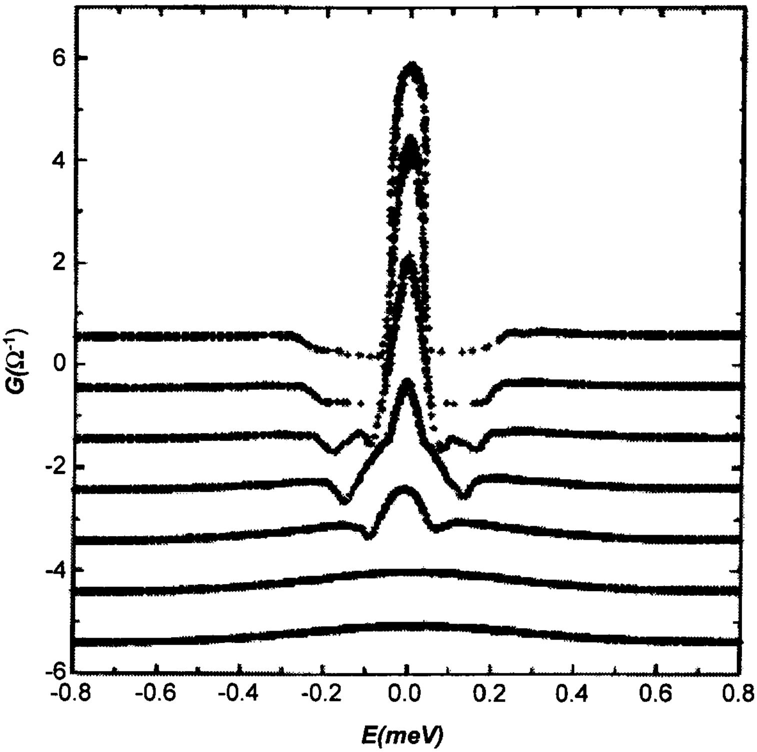

FIGURE 4 The differential conductivity of a UBe_{13}–Au contact junction *versus* energy. Each plot refers to different temperatures $T = 1.09-0.33$ K (bottom to top). The superconducting transition temperature has been estimated to be $T_c = 0.905$ K. Reconstructed from Wälti *et al.*, Ref. [7].

theoretical discussion of Choi *et al.* [20], but in relation to the cuprate superconductors) is that the differential conductivity of UBe_{13}–Au shown in Figure 4 argues strongly against precursor Boson formation in this heavy Fermion superconductor UBe_{13}. This, of course, is to be contrasted with the equally strong evidence in favour of precursor Boson formation in the underdoped cuprate $YBa_2Cu_4O_8$ discussed above (see especially Fig. 3). In particular, analogous tunneling spectroscopy experiments conducted in underdoped single crystals of the high-T_c superconductor $Bi_2Sr_2CaCu_2O_{8+\delta}$ by Renner *et al.* [21] showed indeed the persistence of a gap-like structure (pseudogap) well above the critical temperature. The latter finding is supportive of precursor pairing in the underdoped phase of high-T_c superconductors.

Pertaining to issue (i) set out in Sec. I on the energy scale to be used in relation to $k_B T_c$, it is now going to be helpful in drawing decisive conclusions in this area if high-T_c cuprates could be systematically examined for in-plane data on effective masses m^* and on coherence lengths ξ. Furthermore, should it prove experimentally feasible, high pressure measurements on materials that show strong variation of T_c with pressure [22] would be very valuable, we believe, if m^* and in-plane coherence length ξ could be measured as functions of pressure P for non $-s$-wave paired materials (including heavy Fermions) for which $T_c(P)$ is known.

IV. ENERGY GAP WITH NON-s-WAVE PAIRING

Both heavy Fermion and high-T_c superconductors, together with Sr_2RuO_4 (Ref. [23]), for which the possibility of p-wave superconductivity is still debated [24, 25], are the best known instances of unconventional superconductivity [26, 27]. Such a term is reserved for superconductors characterized not only by the spontaneous breaking of the $U(1)$ symmetry associated with global gauge invariance, but also by the breaking of other symmetries, such as those associated with the crystal point group, or with time reversal invariance. In such cases, the energy gap $\Delta_{\mathbf{k}}$ usually acquires a non-trivial dependence on wave vector $\mathbf{k}$ over the first Brillouin zone of the appropriate reciprocal lattice, at variance with conventional BCS superconductors, where $\Delta_{\mathbf{k}} = \text{const}$. While the proposal of p-wave symmetry superconductivity for most heavy Fermion compounds and for Sr_2RuO_4 is relatively recent, the long controversy about the symmetry of the order parameter in the high-T_c compounds has been resolved only in the last years in favour of d-wave superconductivity, both in hole- and electron-doped compounds, by means of very elegant experiments, aimed at directly probing the phase of the order parameter [28–31]. While both s- and d-wave symmetry require singlet pairing and a complex scalar order parameter (total spin $s = 0$, total relative angular momentum $\ell = 0$ and 2, respectively), p-wave symmetry implies triplet pairing, and requires a vector order parameter [26], as is the case for

^{3}He (see, *e.g.*, Ref. [32]). Given our substantial lack of insight as to the microscopic pairing mechanism of such unconventional superconductors, a detailed knowledge of the **k**-dependence of the energy gap may serve as a clue. Indeed, it was the observation of a frequency dependence in the order parameter that motivated Eliashberg's generalization of BCS theory to embrace strong-coupling superconductors [33]. It has been observed, however, that the sparse evidence for subdominant *s*-wave contributions to $\Delta_{\mathbf{k}}$ in the cuprates, which has been reported to occasionally add to the main *d*-wave contribution, suggests that the symmetry of the order parameter may not be a universal feature, but rather a material specific property, changing within the same class of materials as a function of doping, and possibly even for the same compound, as a function of temperature [34].

At variance with an *s*-wave gap, both *p*- and *d*-wave order parameters may vanish over subsets of the reciprocal lattice vectors. This leads to the existence of nodal manifolds for the energy spectrum $E_{\mathbf{k}} = \sqrt{\xi_{\mathbf{k}} + |\Delta_{\mathbf{k}}|^2}$ in **k**-space, *i.e.*, of (possibly multiply connected) subsets of the reciprocal lattice where $E_{\mathbf{k}} = 0$. Here, $\xi_{\mathbf{k}} = \varepsilon_{\mathbf{k}} - \mu$ denotes the single-particle dispersion relation, measured with respect to the chemical potential μ. Such nodal manifolds are clearly characterized by the simultaneous vanishing of $\xi_{\mathbf{k}}$ and $\Delta_{\mathbf{k}}$, and therefore occur at the intersection between the Fermi manifold (a line, for the quasi-bidimensional cuprates, or a surface, for the three-dimensional heavy Fermion compounds) and the gap nodal manifolds $\Delta_{\mathbf{k}} = 0$ (*e.g.*, $k_y = \pm k_x$ for a *d*-wave cuprate). This may originate in point as well as in line nodes for the superconducting spectrum $E_{\mathbf{k}}$. As a consequence, several typical electronic properties, such as specific heat, thermal conductivity, spin susceptibility, and superfluid stiffness, display a power-law asymptotic behaviour at low temperature, in marked contrast with the 'activated' behaviour in the *s*-wave case, characterized by a nonzero gap Δ over the whole first Brillouin zone. Such power-law behaviours served as a first evidence for unconventional superconductivity both in the cuprates and in the heavy Fermions [35]. It should be then emphasized that the low-temperature behaviour of the elementary excitations in an unconventional superconductor is non trivially governed by the topology of its energy spectrum nodal manifold [36]. Motivated by the observation of pronounced flat zeroes in the energy gap of underdoped Bi-2212 [37], in a way reminiscent of the gapless patches observed above T_c in the same material, as an effect of the existence of a 'pseudogap' in the normal state [38], Angilella *et al.*, have suggested that deviations in the low-energy dependence of the density of states and in the low-T asymptotic behaviour of typical electronic properties may be observed [39].

Modern probes of the detailed structure in **k**-space of the energy gap are provided by angular-resolved photoemission electronic spectroscopy (ARPES) [40]. These gave indeed strong support to the d-wave symmetry character both of the superconducting gap below T_c and of the pseudogap in the normal state of several underdoped cuprates. However, such a technique is best suited for quasi-bidimensional materials, such as the cuprates. Given our aim of comparing and contrasting the properties of a variety of unconventional superconductors as wide as possible, the analysis of the gap magnitude *versus* temperature from tunneling spectroscopy is perhaps more profitful. At variance with ARPES, electronic tunneling spectroscopy does only provide an 'average' information on the energy gap $\Delta(T)$, without yielding direct access to its explicit **k**-dependence. In Figure 5 we show data for the temperature dependence of the normalized energy gap $\Delta(T)$. Measurements refer to electronic tunneling through a UBe_{13}−Au contact junction (open squares) [7], and to a Bi-2212−Nb junction (filled squares) [41]. In both cases, marked deviations from the theoretical BCS curve (solid line) are seen, especially at low temperature. These have been interpreted as evidence for strong coupling in UBe_{13} by Wälti *et al.* [7]. In particular, the measured gaps in both these two non−s-wave superconductors seem to be in better agreement with the asymptotic low-T dependence of $\Delta(T)$, as derived within a generalization of BCS theory for a d-wave order parameter (dashed lines in Fig. 5; see App. B).

IV.1. Gap Anisotropy and Ultrasound Attenuation

To conclude this section on gaps with nodal anisotropy in strongly correlated electron systems, we shall briefly summarize the study of Moreno and Coleman [42] on ultrasound attenuation in such electronic assemblies. As these authors stress, transverse ultrasound attenuation is a versatile probe of electronic gap nodes, and has been

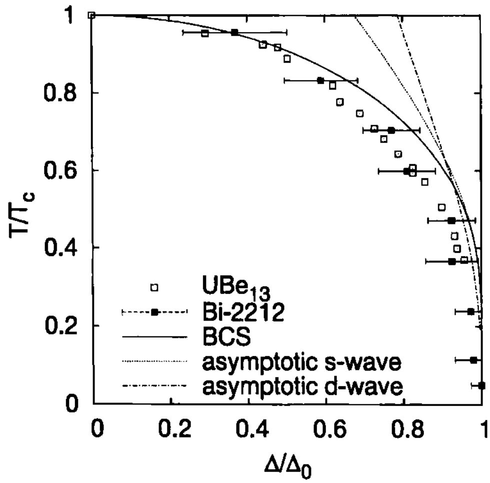

FIGURE 5 T/T_c *versus* $\Delta(T)/\Delta_0$ for the heavy Fermion superconductor UBe_{13} (open squares; data from Wälti *et al.*, Ref. [7]), and for the high-T_c superconductor Bi-2212 (filled squares; data from Lee *et al.*, Ref. [41]). In the former case (UBe_{13}), the zero temperature gap has been extrapolated to agree with $2\Delta_0 = 7k_BT_c$, whereas in the latter case (Bi-2212) Δ_0 actually represents the value of $\Delta(T)$ for the lowest accessed temperature ($T = 4.2$ K, see Ref. [41]). The solid line is BCS *s*-wave curve, whereas the dashed lines represent the asymptotic behaviour for both *s*- and *d*-wave pairing, as indicated (see main text, and App. B).

used in earlier work to locate the gap lines and point nodes in the heavy Fermion superconductor UPt_3 (see Ref. [43]).

Moreno and Coleman [42] note first of all that ultrasound attenuation probes the relaxation of electronic momentum in a model-independent manner. The key element in their interpretation is the viscosity tensor, which has high symmetry with few independent components. Moreno and Coleman [42] devise a theory which connects these components to the location of the gap nodes. As an illustrative example, they consider high-T_c cuprates, and demonstrate the way in which measurements of ultrasound attenuation can provide a fingerprint of gap zeros lying on the diagonal of the first Brillouin zone.

Using a *d*-wave order parameter $\propto \cos(2\theta)$ (see App. B), Moreno and Coleman [42] show that the transverse ultrasound attenuation is $\propto T^{1.5}$ when the wave vector and polarization of the sound wave are parallel to the symmetry axis of the crystal (angle zero). When the angle is $\pi/4$, the temperature dependence is $\propto T^{3.5}$ (see Ref. [42], especially Fig. 2). Graf *et al.* [25] (see also Ref. [44]) have also made proposals concerning the heavy Fermion superconductor UPt_3, which include transverse sound attenuation, again stressing the strong constraints placed on the orbital symmetry of the superconducting order parameter.

V. SUMMARY AND POSSIBLE FUTURE DIRECTIONS

We have here reviewed evidence, both from experiment and theory, bearing on the issues (i) and (ii) set out in Sec. I of this article. We have stressed that out of six heavy Fermion unconventional superconductors, the thermal energy $k_B T_c$ of the four with the lowest values of T_c scales (approximately, of course) linearly with the energy $\hbar^2/(m^*\xi^2)$ formed from the carrier effective mass m^* and the measured coherence length ξ. The ratio $\hbar^2/(m^*\xi^2)$ to $k_B T_c$ is $\sim(1/20)$, indicating the existence of a small dimensionless parameter in this system. But, with the admittedly very sparse experimental data currently available to form $\hbar^2/(m^*\xi^2)$ in CuO_2 planes of the cuprates, it is already clear from Figure 2 that this 'small parameter' is not available in these unconventional superconductors, the ratio of $\hbar^2/(m^*\xi^2)$ to $k_B T_c$ now being, in order of magnitude, near to unity. In spite of the smallness of the corresponding ratio in the unconventional heavy Fermion superconductors considered in Sec. II, the energy gap ratio $\Delta(T)/k_B T_c$ near $T=0$ is in UBe_{13} already almost double the value of the BCS result for s-wave pairing and weak electron-phonon interaction.

The area of defect physics in the superconducting state appears in the process of growth. As but one, very recent, example, individual Zn impurity atoms have had their effects imaged in $Bi_2Sr_2CaCu_2O_{8+\delta}$ by Pan *et al.* [45]. These workers assert that a single impurity atom at a Cu site in one of the CuO_2 planes creates a large perturbation for the strongly interacting electrons in such a plane. They further note their expectation that knowledge of the influence of such an impurity on the superconducting order parameter as well as on the quasiparticle local density of states could afford a testing ground for presently competing theories of high-T_c superconductivity on an atomic scale. Their investigation consisted of scanning tunnelling microscopic observation of such Zn impurity atoms in the high-T_c superconductor $Bi_2Sr_2CaCu_2O_{8+\delta}$. Imaging of the quasiparticle local density of states at such sites has led to the observation of a four-fold symmetric 'quasiparticle cloud' aligned with the *d*-wave gap nodes (compare Sec. IV of the present review).

While the dominant theme of this review has been of electron (hole) liquids flowing through unconventional superconductors, it is appropriate to conclude these proposals as to directions for future study by referring to two studies which, independently, have pointed out that in the underdoped cuprate phase diagram, with very small carrier concentration, there are physical reasons to expect a phase boundary between a carrier (hole) liquid and a Wigner solid. Thus, March *et al.* [46] raised the question as to whether hole solidification could occur in underdoped cuprates. Subsequently, the independent work of Fisher *et al.* [47] (see also Ref. [36], and references therein) has drawn a phase boundary, both sets of workers stressing that this will be a very low temperature phase, because of the ease of melting of Wigner solids (see, *e.g.*, Refs. [48, 49]).

Acknowledgments

One of us (N. H. M.) made his contribution to the present review during a visit to the Physics Department, University of Catania, in the year 2000. Thanks are due to the Department for the stimulating environment and for much hospitality. N. H. M. also wishes to thank Professor V. E. Van Doren for his continuing interest and support. G. G. N. A. acknowledges support from the EU through the FSE program.

References

[1] de Gennes, P. G., *Superconductivity of Metals and Alloys* (Benjamin, New York, 1966).
[2] Gunnarsson, O. (1997). *Rev. Mod. Phys.*, **69**, 575.
[3] Poole, C. P., Farach, H. A. and Creswick, R. J., *Superconductivity* (Academic Press, San Diego, 1995).
[4] Cox, D. L. and Zawadowski, A. (1998). *Adv. Phys.*, **47**, 599.
[5] Sauls, J. A. (1994). *Adv. Phys.*, **43**, 113.
[6] Timusk, T. and Statt, B. (1999). *Rep. Prog. Phys.*, **62**, 61.
[7] Wälti, Ch., Ott, H. R., Fisk, Z. and Smith, J. L. (2000). *Phys. Rev. Lett.*, **84**, 5616.

[8] Angilella, G. G. N., March, N. H. and Pucci, R. (2000). *Phys. Rev. B*, in press.
[9] Uemura, Y. J., Le, L. P., Luke, G. M., Sternlieb, B. J., Wu, W. D., Brewer, J. H., Riseman, T. M., Seaman, C. L., Maple, M. B., Ishikawa, M., Hinks, D. G., Jorgensen, J. D. *et al.* (1991). *Phys. Rev. Lett.*, **66**, 2665.
[10] Egorov, S. A. and March, N. H. (1994). *Phys. Chem. Liquids*, **28**, 141.
[11] March, N. H. (1993). *Phys. Chem. Liquids*, **25**, 65.
[12] Kohno, H. and Yamada, K. (1991). *Progr. Theor. Phys.*, **85**, 13.
[13] Bucher, B., Steiner, P., Karpinski, J., Kaldis, E. and Wachter, P. (1993). *Phys. Rev. Lett.*, **70**, 2012.
[14] Wachter, P., Bucher, B. and Pittini, R. (1994). *Phys. Rev. B*, **49**, 13164.
[15] March, N. H., Pucci, R. and Egorov, S. A. (1994). *Phys. Chem. Liquids*, **28**, 141.
[16] Angilella, G. G. N., March, N. H. and Pucci, R. (2000). *Phys. Chem. Liq.*, in press.
[17] Chiofalo, M. L., Tosi, M. P. and March, N. H. (1999). *Phys. Chem. Liquids*, **37**, 547.
[18] Dai, P., Mook, H. A., Aeppli, G., Hayden, S. M. and Doğan, F. (2000). *Nature*, **406**, 965.
[19] Rossat-Mignod, J. M., Regnault, L. P., Vettier, C., Bourges, P., Burlet, P., Bossy, J., Henry, J. Y. and Lapertot, G. (1991). *Physica C*, **185–189**, 86.
[20] Choi, H.-Y., Bang, Y. and Campbell, D. K. (2000). *Phys. Rev. B.*, **61**, 9748.
[21] Renner, Ch., Revaz, B., Genoud, J.-Y., Kadowaki, K. and Fischer, Ø. (1998). *Phys. Rev. Lett.*, **80**, 149.
[22] Wijngaarden, R. J., Tristan Jover, D. and Griessen, R. (1999). *Physica B*, **265**, 128, and Refs. therein.
[23] Maeno, Y., Hashimoto, H., Yoshida, K., Nishizaki, S., Fujita, T., Bednorz, J. G. and Lichtenberg, F. (1994). *Nature*, **372**, 532.
[24] Mackenzie, A. P. and Maeno, Y. (2000). *Physica B*, **280**, 148.
[25] Graf, M. J., Yip, S.-K. and Sauls, J. A., *cond-mat/0006180*.
[26] Sigrist, M. and Ueda, K. (1991). *Rev. Mod. Phys.*, **63**, 239.
[27] Annett, J. F. (1995). *Contemporary Physics*, **36**, 423.
[28] Van Harlingen, D. J. (1995). *Rev. Mod. Phys.*, **67**, 515.
[29] Kirtley, J. R., Tsuei, C. C., Sun, J. Z., Chi, C. C., Yu-Jahnes, L. S., Gupta, A., Rupp, M. and Ketchen, M. B. (1995). *Nature*, **373**, 225.
[30] Tsuei, C. C. and Kirtley, J. R. (2000). *Phys. Rev. Lett.*, **85**, 182.
[31] Annett, J. F., Goldenfeld, N. and Leggett, A. J., In: *Physical Properties of High Temperature Superconductors*, Edited by Ginsberg, D. M. (World Scientific, Singapore, 1996), **5**.
[32] Leggett, A. J. (1975). *Rev. Mod. Phys.*, **47**, 331.
[33] Scalapino, D. J. (1995). *Phys. Rep.*, **250**, 329.
[34] Koltenbah, B. E. C. and Joynt, R. (1997). *Rep. Prog. Phys.*, **60**, 23.
[35] Annett, J. F., Goldenfeld, N. and Renn, S. R., In: *Physical Properties of High Temperature Superconductors*, Edited by Ginsberg, D. M. (World Scientific, Singapore, 1990), **2**, Chap. 9.
[36] Fisher, M. P. A., In: *Topological aspects of low dimensional systems* (*Aspects topologiques de la physique en basse dimension*), Edited by Comtet, A., Jolicoeur, T., Ouvry, S. and David, F. (Springer Verlag, Berlin, 1999), lecture given at the Les Houches Summer School 1998, session LXIX, cond-mat/9806164.
[37] Mesot, J., Norman, M. R., Ding, H., Randeria, M., Campuzano, J. C., Paramekanti, A., Fretwell, H. M., Kaminski, A., Takeuchi, T., Yokoya, T., Sato, T., Takahashi, T. *et al.* (1999). *Phys. Rev. Lett.*, **83**, 840.
[38] Norman, M. R., Ding, H., Randeria, M., Campuzano, J. C., Yokoya, T., Takeuchi, T., Takahashi, T., Mochiku, T., Kadowaki, K., Guptasarma, P. and Hinks, D. G. (1998). *Nature*, **392**, 157.
[39] Angilella, G. G. N., Sudbø, A. and Pucci, R. (2000). *Eur. Phys. J. B*, **15**, 269.
[40] Randeria, M. and Campuzano, J. C., In: *Models and Phenomenology for Conventional and High-temperature Superconductivity*, Edited by Iadonisi, G.,

Schrieffer, J. R. and Chiofalo, M. L. (IOP, Amsterdam, 1999), **136**, lecture given at the 1997 Varenna International School of Physics "Enrico Fermi", CXXXVI Course, cond-mat/9709107.
[41] Lee, M., Mitzi, D. B., Kapitulnik, A. and Beasley, M. R. (1989). *Phys. Rev. B*, **39**, 801.
[42] Moreno, J. and Coleman, P. (1996). *Phys. Rev. B*, **53**, R2995.
[43] Shivaram, B. S., Jeong, Y. H., Rosenbaum, T. F. and Hinks, D. G. (1986). *Phys. Rev. Lett.*, **56**, 1078.
[44] Graf, M. J., Yip, S.-K. and Sauls, J. A. (1996). *J. Low Temp. Phys.*, **102**, 367.
[45] Pan, S. H., Hudson, E. W., Lang, K. M., Eisaki, H., Uchida, S. and Davis, J. C. (1999). *Nature*, **403**, 746.
[46] March, N. H., Paranjape, B. V. and Siringo, F. (1991). *Phys. Chem. Liquids*, **24**, 131.
[47] Balents, L., Fisher, M. P. A. and Nayak, C. (2000). *Phys. Rev. B*, **61**, 6307.
[48] Parrinello, M. and March, N. H. (1976). *J. Phys. C*, **9**, L147.
[49] Lea, M. J., March, N. H. and Sung, W. (1992). *J. Phys.: Condensed Matter*, **4**, 5263.
[50] Egorov, S. A. and March, N. H. (1994). *Phys. Chem. Liquids*, **27**, 195.
[51] March, N. H., *Electron Correlation in Molecules and Condensed Phases*, Physics of Solids and Liquids (Plenum Press, New York and London, 1996).
[52] Though a and b were obtained directly from ρ_a *vs.* T in Figure 6 as measured by Bucher *et al.* [13], while c and d were found from Figure 3, involving T_1 as well as ρ_a, Eq. (A3) indicates that in the high temperature limit where $T_1 \to t_1$, $t_1 = d/b$. It is also noteworthy that $c/a \simeq d/b \simeq 2.1 \cdot 10^{-4}$ s.
[53] Hussey, N. E., Nozawa, K., Takagi, H., Adachi, S. and Tanabe, K. (1997). *Phys. Rev. B*, **56**, R11423.
[54] Ito, T., Takenaka, K. and Uchida, S. (1993). *Phys. Rev. Lett.*, **70**, 3995.
[55] Zimmermann, H., Mali, M., Brinkmann, D., Karpinksi, J., Kaldis, E. and Rusiecki, S. (1989). *Physica C*, **159**, 681.
[56] Abrikosov, A. A., Gorkov, L. P. and Dzyaloshinski, I., *Methods of quantum field theory in statistical physics* (Dover, New York, 1963).
[57] Gradshteyn, I. S. and Ryzhik, I. M., *Table of Integrals, Series, and Products* (Academic Press, San Diego, 1994), 5th edn.
[58] Einzel, D. and Schürrer, I. (2000). *Physica B*, **284–288**, 451.
[59] Ott, H. R., Rudigier, H., Rice, T. M., Ueda, K., Fisk, Z. and Smith, J. L. (1984). *Phys. Rev. Lett.*, **52**, 1915.
[60] Takigawa, M., Reyes, A. P., Hammel, P. C., Thomson, J. D., Heffner, R. H., Fisk, Z. and Ott, K. C. (1991). *Phys. Rev. B*, **43**, 247.

APPENDIX A: PHENOMENOLOGICAL GENERALIZATION OF TWO-DIMENSIONAL FERMI LIQUID THEORY TO RELATE IN-PLANE RESISTIVITY AND NUCLEAR SPIN-LATTICE RELAXATION TIME IN A PARTICULAR UNDERDOPED HIGH-T_c CUPRATE

In earlier work [15, 50, 51], attention has been drawn to the fact that two-dimensional Fermi liquid theory [12] of electrons (holes) flowing through a CuO_2 plane in an underdoped high-T_c cuprate leads to a simple correlation between in-plane electrical resistivity ρ_a and nuclear spin-lattice relaxation time T_1 of Cu nuclei having the form displayed in Eq. (3) of the main text. As use will be made of the experimental data of Bucher *et al.* [13] on underdoped $YBa_2Cu_4O_8$ below, we reproduce in Figure 6 the experimental results for ρ_a *vs.* T and $(TT_1)^{-1}$ *vs.* T, respectively. It will be important in what follows in this Appendix to note that, well above $T_c \approx 80\,\text{K}$ in this material, one can express ρ_a as

$$\rho_a = a + bT, \quad T \gg T_c, \tag{A1}$$

and, as shown in Figure 3,

$$\rho_a T_1 = c + dT, \quad T \gg T_c, \tag{A2}$$

for T sufficiently large compared with T_c. Equations (A1) and (A2), which we stress again are high temperature limiting forms, are central to the arguments below and therefore we have collected, for the underdoped cuprate studied in the experiments of Bucher *et al.* [13], the values of a to d in Table I. It is relevant here to note the later work by Wachter *et al.* [14], which contrasts the behavior of ρ_a, which represents the intrinsic resistivity of the CuO_2 plane, with the resistivity of the b axis, which is dominated by the chain contribution.

Evidently from Figure 3, the linearity with T shown in Eq. (A2), which is predicted by Fermi liquid theory [15, 50], is limited to high temperatures. The aim of this Appendix is therefore to suggest a phenomenological generalization of this Fermi liquid prediction for all temperatures $T > T_c$ in underdoped cuprates.

To proceed to achieve this objective, we first note from Figure 3 that $\rho_a T_1$ in the regime often called nowadays that of the 'pseudogap' [6, 38] bends upwards from the linear high temperature form Eq. (A2),

TABLE I Best fit to the parameters a to d in the linear approximations Eqs. (A1) and (A2), for ρ_a and $\rho_a T_1$, respectively, as functions of T, for $T \gg T_c$ ($T \geq 250\,\text{K}$). Also included are the values of t_1 and t_2 in Eq. (A3) [52]

$a = 61.3\ \mu\Omega\cdot\text{cm}$
$b = 1.136\ \mu\Omega\cdot\text{cm}\cdot\text{K}^{-1}$
$c = 0.014\ \mu\Omega\cdot\text{cm}\cdot\text{s}$
$d = 2.585\cdot 10^{-4}\ \mu\Omega\cdot\text{cm}\cdot\text{s}\cdot\text{K}^{-1}$
$t_1 = 2.14\cdot 10^{-4}\,\text{s}$
$t_2 = 2.86\ \mu\Omega^{-2}\cdot\text{cm}^{-2}\cdot\text{s}$

whereas from Figure 6, ρ_a itself bends downwards. To examine this behavior further, we note first from Figure 6 that whereas $(TT_1)^{-1}$ has a maximum *vs.* T, ρ_a *vs.* T is monotonic, and can therefore be inverted to obtain $T_1 \equiv T_1(\rho_a)$, for $T > T_c$. After some exploratory work, we converged on a rather simple representation of this functional form as

$$T_1 = t_1 + \frac{t_2}{\rho_a^2}, \tag{A3}$$

which is shown in Figure 7. This gives the clue to what we are seeking, namely to generalize phenomenologically the high-temperature Fermi liquid linearity for $\rho_a T_1$ displayed in Figure 3 to embrace the 'pseudogap' regime of T near to T_c.

Equation (A3) immediately focusses on the product $\rho_a^2 T_1$ as the quantity to use in seeking such a phenomenological generalization of Eq. (A2). To gain orientation, let us next multiply the high temperature limits in Eqs. (A1) and (A2) to obtain

$$\rho_a^2 T_1 = e + fT + gT^2, \tag{A4}$$

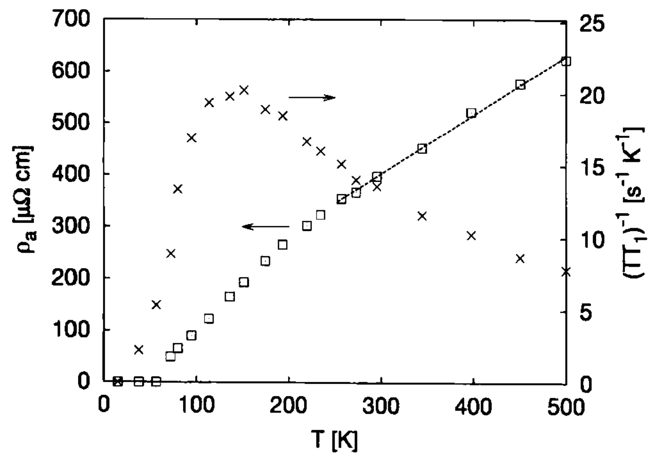

FIGURE 6 In-plane resistivity ρ_a (left scale, squares) and nuclear spin-lattice relaxation time T_1 of Cu nuclei (right scale, crosses) as functions of temperature T for underdoped $YBa_2Cu_4O_8$ (after Bucher *et al.*, Ref. [13]). Quantity actually plotted on ordinate (right scale) is $(TT_1)^{-1}$. Note the good linear fit for $\rho_a(T)$ at $T \gg T_c$ by Eq. (A1), with a and b as recorded in Table I.

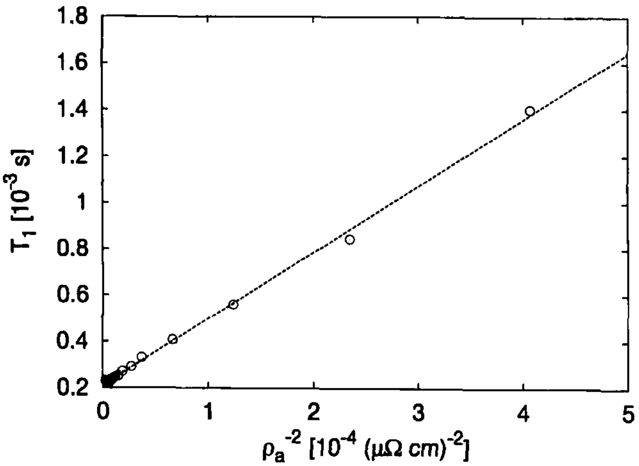

FIGURE 7 Plot of T_1 *vs.* ρ_a^{-2}, obtained by inverting $\rho_a(T)$ relation of Figure 6 and converting thereby $T_1(T)$ of Figure 6 into $T_1(\rho_a)$. Circles show experimental points and dashed line is linear approximation. Note that aim of this figure is to motivate plot of Figure 8.

and we take this to be, therefore, the rather natural phenomenological generalization of the Fermi liquid high temperature result, Eq. (A2), for underdoped high T_c cuprates. Unfortunately, as the proposal (A4) stands, it appears to require the determination from experiment of three parameters e, f and g.

Therefore, the natural first step seemed to be to plot the 'asymptotic' high temperature product $\rho_a^2 T_1$, formed from simply taking the product of Eqs. (A1) and (A2), and such a plot is shown in Figure 8. What is immediately apparent is that this 'apparently asymptotic' result works well right down through the 'pseudogap' region. The conclusion is clear: The parameters e, f and g in the proposed 'quadratic' phenomenological generalization of Eq. (A4) of the Fermi liquid high temperature limit in Eq. (A2) are completely determined by the constants a to d recorded in Table I. The relations are evidently:

$$e = ac, \tag{A5a}$$

$$f = ad + bc, \tag{A5b}$$

$$g = bd. \tag{A5c}$$

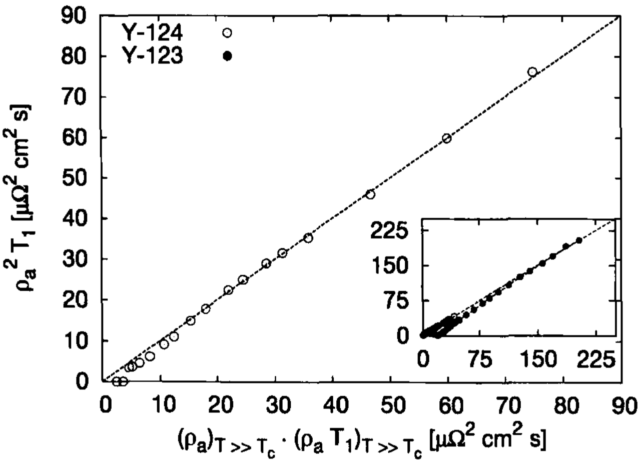

FIGURE 8 Plot of combination $\rho_a^2 T_1$ (see Eq. (A4) and Fig. 7) *vs.* quadratic function of temperature for $YBa_2Cu_4O_8$, the independent variable $(\rho_a^2 T_1)_{T \gg T_c}$ using only the parameters *a* to *d* in Table I. Data for ρ_a are from Bucher *et al.* (Ref. [13]), while data for T_1 are from Zimmermann *et al.* (Ref. [55]). The straight line $\rho_a^2 T_1 = (\rho_a^2 T_1)_{T \gg T_c}$ is a guide to the eye (*no fit*), which emphasizes the linear correlation at all temperatures discussed in App. A. The inset shows the same quantities of the main plot again for $YBa_2Cu_4O_8$ (open circles), this time with data for ρ_a taken from Hussey *et al.* (Ref. [53]), and for $YBa_2Cu_3O_{7-\delta}$, over a wider range in temperature (filled circles; data for ρ_a are from Ito *et al.*, Ref. [54], while data for T_1 are from Takigawa *et al.*, Ref. [60]). The dashed lines are guides to the eye. While the correlation discussed in App. A is confirmed for $YBa_2Cu_4O_8$ by the analysis of this new set of data, the same result seems not to hold for $YBa_2Cu_3O_{7-\delta}$ over the whole temperature range investigated experimentally.

In short, though the 'pseudogap' regime is often spoken about as containing a basically new mechanism from the high temperature regime, what is demonstrated here is that the product $\rho_a^2 T_1$, which is evidently a basic combination of in-plane resistivity ρ_a and nuclear spin-lattice relaxation time T_1, requires no new information content beyond the high temperature limits, Eqs. (A1) and (A2), for ρ_a and $\rho_a T_1$, respectively, to extend it through the 'pseudogap' regime.

What we stress here is that Eq. (A4) represents the data of Bucher *et al.* [13] on $YBa_2Cu_4O_8$ using information on the right-hand side, which contains knowledge only of high-temperature properties. It seems remarkable that in this particular material, while ρ_a and T_1 separately have clear fingerprints individually of the so-called 'pseudogap' regime, such pseudogap information does not appear in the combination $\rho_a^2 T_1$ in Eq. (A4).

We must point out that Eq. (3) rests on the assumption that both ρ_a and T_1 can be written in terms of the susceptibility $\chi(\mathbf{Q})$ at some assumed dominant antiferromagnetic wave vector $\mathbf{Q}$. In fact, since T_1 fundamentally depends on the imaginary part of $\chi(\mathbf{q}, \omega)$, one strictly wants more detail about the susceptibility in each underdoped cuprate considered. For a further example we have treated, the simple phenomenology that works so convincingly for underdoped $YBa_2Cu_4O_8$ will need generalizing to include experiments on susceptibility. This is indicated in the inset of Figure 8, where we have repeated the above considerations for another set of data for ρ_a in $YBa_2Cu_4O_8$ (Hussey *et al.*, Ref. [53]), and for the compound $YBa_2Cu_3O_{7-y}$ (Ito *et al.*, Ref. [54] for ρ_a; Zimmermann *et al.*, Ref. [55] for T_1). While our proposal is confirmed again in $YBa_2Cu_4O_8$, the correlation discussed in this Appendix seems to fail for $YBa_2Cu_3O_{7-y}$.

APPENDIX B: ASYMPTOTIC LOW-*T* GAP DEPENDENCE FOR A *d*-WAVE SUPERCONDUCTOR

One of the most celebrated goals of BCS theory was that of providing a universal (tanh-like) law for the T-dependence of the gap energy $\Delta(T)$ below T_c. Small deviations from such a law were observed already in conventional superconductors near T_c, and may be attributed to depairing effects, which are believed to become stronger as T_c is approached from below. Such depairing effects are expected to be operative also in unconventional superconductors. Moreover, especially in the case of underdoped high-T_c superconductors, the proximity to the normal state, characterized by a 'pseudogap', may contribute with yet different sources of deviations from the predicted BCS law, $\Delta(T) \sim (1 - T/T_c)^{1/2}$, as $T \to T_c$. That is why a departure from the conventional BCS curve as $T \to 0$, as observed in both UBe_{13} and Bi-2212 (compare Fig. 5), can be more likely traced back to an effect of strong coupling.

In order to derive the asymptotic low-T dependence of the gap function for a d-wave superconductor, one may follow the standard textbook procedure [56]. However, in doing so, one has to retain the anisotropic $\mathbf{k}$-dependence of the gap as far as needed. Assuming $\Delta = \Delta(T) g(\theta)$, where θ is an angular coordinate over the Fermi line, assumed to be closed around the Γ point in the first Brillouin zone, and $g = g(\theta) \sim \cos(2\theta)$ for a d-wave superconductor, one straightforwardly obtains:

$$\frac{\Delta(T)}{\Delta_0} \sim 1 - \frac{1}{\langle g^2 \rangle_{\rm FS}} \left\langle g^2 \sqrt{\frac{2\pi k_{\rm B} T}{\Delta_0 |g|}} \exp(-\Delta_0 |g| / k_{\rm B} T) \right\rangle_{\rm FS}, \quad T \to 0 \quad \text{(B1)}$$

to first order in $k_{\rm B}T/\Delta_0$. Here, $\langle \cdots \rangle_{\rm FS} = \int_0^{2\pi} d\theta \cdots$ denotes an average over the Fermi line. For $g(\theta) \equiv 1$, one recovers the familiar expression valid for s-wave superconductors [56].

Performing the integration for the d-wave case, one analytically obtains:

$$\begin{aligned} \delta(x) = \frac{2}{\Gamma(7/4)} \sqrt{\frac{2}{x}} \Bigg(\Gamma\left(\frac{5}{4}\right) {}_1F_2\left[\frac{5}{4}, \left\{\frac{1}{2}, \frac{7}{4}\right\}, \frac{1}{4}x^2\right] \\ - x \frac{\Gamma^2(7/4)}{\Gamma(9/4)} {}_1F_2\left[\frac{7}{4}, \left\{\frac{3}{2}, \frac{9}{4}\right\}, \frac{1}{4}x^2\right] \Bigg), \end{aligned} \quad \text{(B2)}$$

where $\delta = 1 - \Delta(T)/\Delta_0$, $\Delta_0 = \Delta(T=0)$, $x = \beta\Delta_0 = \Delta_0/k_{\rm B}T$, $\Gamma(z)$ is Euler's gamma function, and ${}_pF_q[\{a_1, \ldots, a_p\}, \{b_1, \ldots, b_q\}, z]$ is the generalized hypergeometric function [57].

The ratio of Δ_0 to $k_{\rm B}T_c$ agrees with the formula:

$$\frac{\Delta_0}{\pi k_{\rm B} T_c} = \exp(-\gamma_\ell), \quad \ell = s, d, \quad \text{(B3)}$$

where $\gamma_s = \gamma = 0.57721\ldots$ (Euler's constant), while [58]

$$\gamma_d = \gamma + \frac{\langle g^2 \log |g| \rangle_{\rm FS}}{\langle g^2 \rangle_{\rm FS}} = \gamma + \frac{1}{2}(1 - 2\log 2) = 0.384068\ldots, \quad \text{(B4)}$$

for the s- and d-wave cases, respectively. Equation (B2) has been used to construct the low-T d-wave asymptote in Figure 5.

APPENDIX C: INTEGRATED SPECIFIC HEAT RELATED TO REDUCED GAP δ

The purpose of this Appendix is to compare results relating specific heat and gap parameter for the non-s-wave heavy Fermion superconductor UBe_{13} with the corresponding BCS predictions. The work of Ott *et al.* [59] on the specific heat of UBe_{13} will be combined with the experimental results of Wälti *et al.* [7], which we have already discussed at some length in Sec. III.2 (see also App. B). In Figure 9 we show the electronic specific heat C^{es} in the superconducting state normalized with γT_c, where $\gamma T_c = C^{en}(T_c)$ in the normal state. The results of Ott *et al.* [59] for UBe_{13} are compared with the prediction of BCS theory. The measurements are of the specific heat C_P at constant pressure. The inset shows the integrated specific heat

$$\varepsilon(T) = \int_0^T \frac{C^{es}}{\gamma T_c} d\left(\frac{T}{T_c}\right), \tag{C1}$$

and though Ott *et al.* [59] emphasized the deviations of their measurements from the BCS form, it can be seen that there are similarities, but that there is a crossing of the two curves with the present normalization, for $T/T_c \gtrsim 0.8$.

Figure 10 then shows the combination of the data presented in Figure 9 with the reduced gap parameter $\delta = 1 - \Delta/\Delta_0$. Actually, whereas the continuous curve displaying the BCS theory prediction

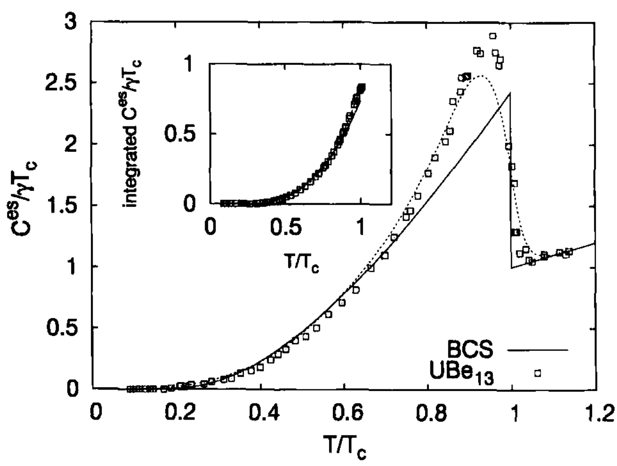

FIGURE 9 Electronic specific heat and integrated electronic specific heat [inset; Eq. (C1)] *versus* reduced temperature T/T_c for UBe_{13} at constant pressure (data from Ott *et al.*, Ref. [59]) and for BCS theory at constant volume. Dashed lines are guides to the eye.

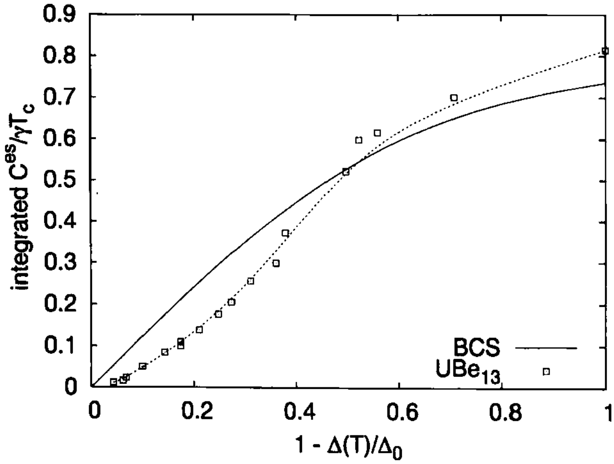

FIGURE 10 Plots 'integrated specific heat' $\varepsilon(T)$ [Eq. (C1)] *versus* reduced gap $\delta(T) = 1 - \Delta(T)/\Delta_0$. Points refer to combined data for $\Delta(T)$ (from Wälti *et al.*, Ref. [7]) and specific heat (Ott *et al.*, Ref. [59]; see also Fig. 9 above) for UBe_{13}. The dashed line is a guide to the eye. The continuous line represents BCS theory for s-wave superconductors. For the non$-s$-wave case of UBe_{13}, the slope at the origin seems to go to zero and also there is a point of inflection. Both of these features differ from the BCS s-wave curve.

comes out from the origin with finite slope, the 'experimental' points of Figure 10 suggest that the slope at the origin is zero in this non$-s$-wave material. The origin of the finite slope at $T = 0$ in the BCS curve can be ultimately traced back to the asymptotic low-T behaviours of $\Delta(T)$ [compare Eq. (B1)], and of the integrated specific heat, which before integration behaves as:

$$C_V \sim (\beta\Delta_0)^{3/2} \exp(-\beta\Delta_0), \quad T \to 0. \tag{C2}$$

Both quantities contain an exponentially 'activated' prefactor, and a factor $\propto T^{n/2}$ with n integer. It will, we believe, be interesting to see if there is any 'universality' of behaviour in such a plot when further data becomes available for the non$-s$-wave superconductors that are the focus of the present article.